Available online at www.sciencedirect.com

ScienceDirect

journal homepage: www.elsevier.com/locate/he

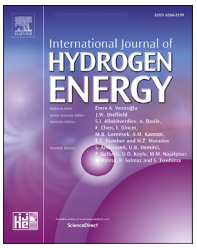

Numerical and experimental investigation of hydrogen enrichment in a dual-fueled CI engine: A detailed combustion, performance, and emission discussion

Upendra Rajak [a], *Prerana Nashine* [b], *Tikendra Nath Verma* [c,**], *Ibham Veza* [d], *Ümit Ağbulut* [e,*]

[a] *Department of Mechanical Engineering, RGM College of Engineering and Technology Nandyal, Andhra Pradesh, 518501, India*

[b] *Department of Mechanical Engineering, National Institute of Technology, Rourkela, 769008, India*

[c] *Department of Mechanical Engineering, Maulana Azad National Institute of Technology Bhopal, Madhya Pradesh, 462003, India*

[d] *Department of Mechanical Engineering, Universiti Teknologi PETRONAS, 32610 Bandar Seri Iskandar, Perak Darul Ridzuan, Malaysia*

[e] *Depermant of Mechanical Engineering, Faculty of Engineering, Düzce University, 81620, Düzce, Türkiye*

HIGHLIGHTS

- The effects of combining hydrogen (5.0%) with diethyl ether, n-butanol, and a diesel blend were studied.
- Direct diesel compression ratios have an impact on performance and emissions.
- Because 5H295DEE has the highest cetane number, it has the smallest ignition delay.
- The findings revealed that as the proportion of H_2 in the mixtures grew, NO_X emissions increased as well.

ARTICLE INFO

Article history:
Received 13 April 2022
Received in revised form
12 July 2022
Accepted 18 July 2022
Available online xxx

Keywords:
Compression-ignition engine
Biofuels
Hydrogen
Engine performance
Particulate matter

ABSTRACT

An effort has been made to simulation a compression ignition engine using hydrogen-diesel, hydrogen-diethyl ether, hydrogen-*n*-butanol and base diesel fuel as alternatives. The engine measured for the simulation is a single cylinder, four stroke, direct injection, diesel engine. During the simulation the injection timing and engine speed are kept constant at 23°bTDC and 1500 rpm. Diesel-RK, a piece of commercial software employed for this project, can forecast an engine emission, performance and combustion characteristics. The examination of the anticipated outcomes reveals that adding hydrogen to diesel leads in a small increase in efficiency and fuel consumption. With the usage of hydrogen-blend fuels, the majority of dangerous pollutants in exhaust are greatly decreased. The shortest ignition delay was consistently given by 5H295DEE. The lowest CO_2 (578.61 g/kWh) was given by 5H295nB at CR 19.5. Hydrogen blends increase NOx emissions more than base diesel fuel. In the case of smoke and particulate matter emission, the reduce tendency was seen.

* *Corresponding author.*
** *Corresponding author.*
E-mail addresses: tnverma@manit.ac.in (T.N. Verma), umitagbulut@duzce.edu.tr (Ü. Ağbulut).

https://doi.org/10.1016/j.ijhydene.2022.07.144
0360-3199/

Introduction

The use of biodiesel-hydrogen blends has attracted considerable attention due to substantial improvement in diesel engine presentation, combustion, and discharge physiognomies. A dual-fuel machine with hydrogen fumigation was employed by Dimitriou et al. [1] to reduce NOx emanations. The outcomes displayed that biodiesel-hydrogen enabled the engine to be operated with increased EGR rates without penalty for soot emissions. Higher EGR rates could reduce NOx emission significantly up to 64% with HC and CO also decreased. Furthermore, since higher EGR rates led to stoichiometric combustion, a reduction in the BTE could also be avoided at little and average loads. By advancing the ignition phasing, the efficiency could be improved for the biodiesel-hydrogen engine; while soot, HC, and CO emanations were successfully reduced with moderate NOx enhancement levels. Kanth and Debbarma [2] used a 10% and 20% blend of rice bran and Karanja oil biodiesel with supplemented hydrogen at 7 L/min. It was found that hydrogen enrichment could increase BTE by 2–6%, while fuel consumption was successfully reduced. Moreover, the presence of H_2 decreased the CO and HC emissions by 7–35%. Overall, in the presence of hydrogen, rice bran oil showed superior results to Karanja biodiesel. Loganathan et al. [3] The effect of diethyl ether on hydrogen-enriched cashew nut shell (CNS) oil was investigated, and it was discovered that H_2 enrichment with CNS oil did not affect liquid B20, but could increase the BTE and reduce the CO and HC emissions. The vibration of a vehicle is also a substantially important aspect of passengers' safety and comfort. Hydrogen enrichment could improve the vehicle vibration characteristic to some extent. In a study, Çalık [4] investigated the vibration behaviors of a diesel engine by diesel and alternative fuels enriched with hydrogen. It was found that the use of a diesel-alternative mixture could decrease the vibration of the engine block. Furthermore, by adding hydrogen, further reduction of engine vibration was successfully achieved. Khan et al. [5] attempted to clarify the effect of biodiesel and oxy-hydrogen (HHO) gas enrichment on a 315 cc compression ignition engine and found that oxy-hydrogen enriched diesel could increase the power and torque significantly, while the oxy-hydrogen enriched biodiesel gave contrary results on the engine efficiency. diesel-alternative mixture H_2 enrichment at 2.81 L/min boosted power and torque by over 3%. It also increased diesel BTE by approximately 4%. Premature combustion caused by high CCI biodiesel fuel and HHO resulted in a 2.97% drop in BTE compared to B5. So B5 was thought to be the best fuel for this investigation. The addition of nanoparticles to hydrogen-biodiesel is also an interesting topic. Manigandan et al. [6] investigated the addition of zinc oxide and titanium dioxide nanoparticles with hydrogen-biodiesel. The brake power was found to increase by 22% and 4% using titanium dioxide and zinc oxide, respectively. Reductions by 18% and 15% in BSFC at 50% engine load were also observed. Additionally, titanium dioxide and zinc oxide addition to hydrogen-biodiesel reduced HC emission by 37% and 26%, CO emissions by 26% and 36%, NOx emissions by 19% and 15%, and smoke opacity by 13% and 8%, respectively. Combining diesel-biodiesel-silver thiocyanate nanoparticles-hydrogen peroxide, Elkelawy et al. [7] found that the AgSCN (SCP**1**)Nanoparticles/H_2O_2 emulsion could improve the combustion process with significant lower NOx emissions.

Glycerol waste, a by-product of alternative production, can be used to produce hydrogen. Saidi and Moradi [8] used membrane technology to model glycerol steam reforming. Glycerol conversion was expedited by increasing operating temperature and pressure, but it was retarded by a tall feedstuff molar and arc ratio. From 350 to 500 °C, hydrogen recovery improved from 70% to 95% with a feed molar ratio of 3. Increasing the arc ratio from 0 to 20 with 350 °C at 1 bar increased hydrogen recovery from 50% to 71%. Note that despite the potential of biodiesel-hydrogen blends as biofuel, biodiesel itself is susceptible to oxidation. In storage and transportation, it is also prone to produce insoluble which may change some key fuel properties [9]. For that reason, partial hydrogenation is a promising approach to improve biodiesel's corrosion constancy and taciturn movement belongings [10]. Using fractional hydrogenation of unsaturated FAME (H-FAME), Sukjit et al. [11] tried to improve the tribological characteristic of palm biodiesel. The results indicated that the molecules of *Cis*-unsaturated found in H-FAME could produce a lubricating film that was stable and strong. Furthermore, the unsaturated molecules decrease in H-FAME was found to reduce the sensitivity to humidity. H-FAME was also observed to decrease the severity of corrosive and abrasive wear with deposits agglomeration decreased as a result of using fractional hydrogenation of unsaturated fatty acid methyl esters. Meng et al. [12] examined the Bell-Evans-Polanyi (BEP) associations for hydrogen concept responses by H and OH radicals, aiming to provide speedy estimation with satisfactory accuracy to several kinetic aspects of biodiesel combustion. The results revealed that the developed BEP correlations could estimate biodiesel molecules thermochemical data accurately with a substantial reduction in computation load, thus facilitating the kinetic model development of biodiesels. Chacko et al. [13] studied engine combustion and emissions with hydrogenation and EHN addition. Despite its energy-intensive process, the fractional hydrogenation provided improved BSFC-NO_X-smoke trade-off attributes compared to the EHN. To improve the hydrogenation of biodiesel, Zhu et al. [14] $[Ni(NH_3)_6](NO_3)_2$ as a precursor in an amalgamated bentonite-based nickel catalyst. Using such a method, they found that the Ni crystallite aggregation on the catalyst was able to be significantly inhibited with enhancement in the combination of bentonite and nickel. The authors argued that the $[Ni(NH_3)_6](NO_3)_2$ anchoring on bentonite played an important role in facilitating the catalyst activity for the Jatropha biodiesel hydrogenation.

Ammonia is a good hydrogen transporter that may be utilized by hydrogen for better ignition. Wang et al. [15] discovered that adding H_2 to ammonia might increase the laminar flame velocity and reduce NOx emission in a marine compression ignition engine. Natural gas has recently gained popularity for use in internal combustion engines due to its low cost, high octane number and high hydrogen carbon ratio. Wang et al. [16] examined the combustion phasing of a diesel-natural gas hybrid engine. The results demonstrated that diesel injection time influenced the entire combustion

Please cite this article as: Rajak U et al., Numerical and experimental investigation of hydrogen enrichment in a dual-fueled CI engine: A detailed combustion, performance, and emission discussion, International Journal of Hydrogen Energy, https://doi.org/10.1016/j.ijhydene.2022.07.144

process. The pilot CI injection was advanced to reduce the natural gas combustion time from 35.5° to 16.5°CA. The shorter ignition duration of natural gas may have been attributed to its reduced specific energy consumption. The use of butanol in internal combustion engines shows a great promise [17–19], but the combination of diesel fuel with biodiesel, butanol and hydrogen needs further investigation. Saleh [20] on a direct injection compression ignition engine, we used diesel-jojoba oil-butanol mixed with hydrogen peroxide. Results revealed that the blend with 5% by jojoba oil-8% by butanol (DJ5B8) gave the greatest presentation in terms of BSFC, EGT and BTE. When 5% of hydrogen bleach was added toward the DJ5B8, further improvement was achieved [34,35].

Although a number of studies have endeavored to clarify the consequence of hydrogen amelioration in diesel locomotives fueled with biodiesel, most previous works in the literature were conducted using edible biodiesel. The use of non-food-based biodiesel enriched with hydrogen is therefore worth further investigation. This study investigates adding hydrogen energy sharing in a single-cylinder diesel-engine fueled by 5% hydrogen enrichment with diesel, diethyl ether, and n-butanol for higher load with varied compression ratios using three distinct ways. The simulated techniques include (a) adding hydrogen to the diesel fuel, (b) adding hydrogen to the diethyl ether, and (c) adding hydrogen to the n-butanol. Using numerical techniques and the Diesel RK Model Software, this study aims to maintain engine load, extend diesel engine performance, and reduce pollutants while decreasing hydrogen energy and fuel consumption.

Materials and methods

In this investigation, four samples were used to generate basic diesel fuel blends: diesel, hydrogen, diethyl ether (DEE), and n-butanol. First, a 95% fraction of base diesel with 5% hydrogen energy (5H295BD), then a 95% fraction of diethyl ether with 5% hydrogen energy (5H295DEE), and finally a 95% fraction of n-butanol with 5% hydrogen energy (5H295nB), all of which were compared to the base diesel fuel. Using a single-cylinder four-stroke diesel-engine, the numerical tool of the Diesel RK-Model programmed was utilized to compare these fraction mixes. The characteristics of several fuel samples are listed in Table 1. The fraction of hydrogen dynamism in the energy assortment can be premeditated by Eq. (1) [36,37]. With a 5% hydrogen energy contribution, diesel, diethyl-ether, and n-butanol are used in this study.

$$Hydrogen\ energy\ share = \frac{Mass\ flow\ rate\ of\ H_2 \times LHV\ of\ H_2}{Mass\ flow\ rate\ of\ H_2 \times LHV\ of\ H_2 + Mass\ flow\ rate\ of\ diesel \times LHV\ of\ diesel} \quad (1)$$

Table 1 – ASTM standards were used to measure the properties of various fuels.

Property	Diesel	Hydrogen	Diethyl ether	n-butanol
Viscosity, (mm^2/s) at 40 °C	3.80	0.0083	0.23	2.2
Flash-point, (°C)	61.2	585	−45	36
Density, (kg/m^3) at 15 °C	838.0	0.084	713.0	810.0
Calorific value, (MJ/kg)	43.1	119–120	33.9	34.0
Cetane number	45–55	5–10	125.0	25.0

Engine system and test procedure

Completely of the tests were accepted out on a single-cylinder, 4-stroke, direct-injection diesel engine at an influence output of 3.5 kW with rpm of 1500. The technical minutiae and schematic of the test machine arrangement were depicted in Table 2 and Fig. 1. Correspondingly. The engine is linked to an AC dynamometer to deliver brake load. The test combinations were inserted directly into the ignition cylinder through the prevailing injection arrangement at constant fuel injection pressure and temperature. A solenoid-controlled automated burette between the fuel pump and the machine energy chamber, as well as a differential pressure feeler in the air box, were used to assess air utilization. An outpouring container dampens engine vibrations and maintains stable airflow through the intake manifold. To ration the in-cylinder gas pressures, a piezoelectric-pressure feeler (Kistler) was tight-fitted to the cylinder head and linked to a charge amplifier. The heat release rates were calculated using 1D thermodynamic models grounded on the unhurried chamber pressure. Fig. 1 depicts the numerical and experimentally obtained in-cylinder pressure and NOx emission under various compression ratios at 1500 rpm and 3.5 kW. It is clear that the numerical results are in excellent agreement with the experimental data, particularly when the diesel is fueled with CR17.5.

The prepared fuel blends are tested under various engine loads. Preliminary to each test, the engine is run with BD100

Table 2 – Engine operating parameters.

Bore, stroke	87.5 mm, 110 mm
Connecting rod length	234.0 mm
Compression ratio	15.5–19.5
Cooling method	water
Model	TV1
Connecting Rod length	234 mm
Rate speed	1500 rpm
Swept Volume	661.45 (cc)
Fuel type	Diesel, biodiesel, and hydrogen

Please cite this article as: Rajak U et al., Numerical and experimental investigation of hydrogen enrichment in a dual-fueled CI engine: A detailed combustion, performance, and emission discussion, International Journal of Hydrogen Energy, https://doi.org/10.1016/j.ijhydene.2022.07.144

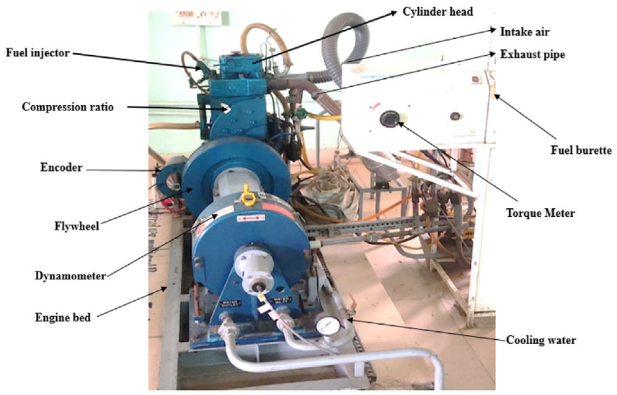

Fig. 1 – Engine under test.

Table 3 – Parameter uncertainty.

Parameter	Uncertainty
Smoke meter	±1.0%
Speed indicator	±1.0%
Temperature	±0.15%
Pressure transducer	±0.5%
NO_X	±0.5%
Load gauge	±0.2%
Heat value measurement	±1.0%
Crank Angle encoder	±0.2%
CO_2	±1.0%
Burette fitted measurement	±0.5%

for 15 min to make sure the dependability of attained statistics. The experiment values are taken after the engine reached a steady-state condition. All tailpipe exhausts are evaluated in a real-time manner using the AVL444 exhaust gas analyzer.

Experiment uncertainty

Experimental uncertainties can happen for a variety of reasons. The uncertainties instigated by instruments second-hand to test countless strictures throughout the study is one of them. If $\mu_1, \mu_2 \ldots \mu_n$ are allied uncertainties through separate strictures, Eq. evaluations the entire uncertainties (μ) of the experimentation (2). Table 3 [23,38,39] shows the parameter estimation errors. Table 3 shows the uncertainties of all measured measurements. There was a total uncertainty of 2.2% in the testing.

Uncertainty (μ) = Square root of [(uncertainty of CP sensor)^2 + uncertainty of power)^2 + uncertainty of fuel consumption)^2 + (uncertainty of temperature sensor)^2 + (uncertainty of ID)^2 + (uncertainty of HRR)^2 + (uncertainty of smoke meter)^2 + (uncertainty of H_2-)^2 + (uncertainty of air flow)^2 + (uncertainty of speed)^2 + (uncertainty of crank encoder)^2]. (2)

Uncertainty (μ) = Square root of $[(0.5)^2 + 0.5)^2 + 0.5)^2 + (0.15)^2 + (0.7)^2 + (1.0)^2 + (1.0)^2 + (0.5)^2 + (0.5)^2 + (1.0)^2 + (0.2)^2]$.

Combustion analysis

In the Diesel-RK program, thermodynamic models that are based on the first law of thermodynamics are utilized to examine engine performance characteristics. Temperature, heat release rate, pressure, ignition delay, and other necessary characteristics are assessed in relation to crank angle or in relation to time. Semi-empirical correlations drawn from experimental findings are used to account for the engine friction and heat transmission. Multi-zone modeling is used to replicate the engine's internal combustion process. The following conservation equations from Fiveland and Assanis are accounted for in the model [40].

Equations in the Diesel-RK software

The mass fraction evaluation and destruction of each species are part of the species conservation equations (3)–(8) [22,40–42].

$$\frac{dm}{dt} = \sum_j \dot{m}_j \tag{3}$$

$$Y_i = \frac{m_i}{m} \tag{4}$$

$$\frac{d(mY_i)}{dt} = \sum_j \dot{m}_j Y_i^j + \dot{S}_g \tag{5}$$

$$\dot{S}_g = \frac{m_i}{m} \cap_i W_{mw} V \tag{6}$$

$$\dot{Y}_i = \sum_j \left(\frac{\dot{m}_j}{m}\right)\left(Y_i^j - Y_i^{cyl}\right) + \frac{\cap_i W_{mv}}{\rho} \tag{7}$$

$$\frac{d(mu)}{dt} = -P\frac{dv}{dt} + \frac{dQ_{ht}}{dt} + \sum_j \dot{m}_j h_j \tag{8}$$

Equation (8) shows energy conservation. The left side represents the system's energy change rate. The one, two, and three footings on the accurate indicate movement-effort, heat-transfer and enthalpy-flow.

$$\alpha_i = \frac{(A/F)}{(A/F)} = \frac{\left(\dot{m}_a/\dot{m}_f\right)}{\left(\dot{m}_a/\dot{m}_f\right)_s} \tag{9}$$

$$FMEP = \alpha + \beta P_{max} + \gamma V_p \tag{10}$$

$$SFC = \frac{\dot{m}_j}{P_b} \tag{11}$$

It is the proportion of real to stoichiometric air-fuel proportion in equation (9). As illustrated in the equation, the FMEP is determined (10). The BSFC equation is by way of follows: (11). Because the burning of energy in an IC machine happens in stages, the following governing equations 12–15 are used to compute heat release in the cycle in this model.

(1) Delay phase of ignition:

Please cite this article as: Rajak U et al., Numerical and experimental investigation of hydrogen enrichment in a dual-fueled CI engine: A detailed combustion, performance, and emission discussion, International Journal of Hydrogen Energy, https://doi.org/10.1016/j.ijhydene.2022.07.144

The following formula is used to calculate the auto ignition delay period:

$$\tau = 3.8 \times 10^{-6}\left(1 - 1.6 \times 10^{-4}.n\right)\sqrt{\frac{T}{P}}\exp\left(\frac{E_a}{8.312T} - \frac{70}{CN + 25}\right) \quad (12)$$

(2) A phase of premixed-combustion:

During the premixed-combustion period, the HRR is increased thru:

$$\frac{dx}{d\tau} = \varphi_0 \times \left(A_0\left(m_f/V_i\right) \times (\sigma_{ud} - X_0) \times (0.1 \times \sigma_{ud} + X_0)\right) + \varphi_1 \times \left(\frac{d\sigma_u}{d\tau}\right) \quad (13)$$

(3) Controlled combustion period of mixing:

The HRR during the mixing regulated ignition stage can be calculated as follows:

$$\frac{dx}{d\tau} = \varphi_1 \times \left(\frac{d\sigma_u}{d\tau}\right) + \varphi_2 \times \left(A_2\left(m_f/V_c\right) \times (\sigma_u - X) \times (\alpha - X)\right) \quad (14)$$

The HRR throughout the late burning stage period is provided by:

$$\frac{dx}{d\tau} = \varphi_3 A_3 K_T (1 - X)(\alpha\varepsilon_b - X) \quad (15)$$

There is a period equation for each of these four phases. Constants φ0 = φ1 = φ2 = φ3 = over time, these functions describe the completion of fuel vapour combustion.

The chain Zeldovich technique is used to determine the thermal NO, as shown in equations 16 and 17. The set of equations also comprises fourteen-symmetry calculations, three material balance equations, and three material balance equations, in addition to the Dalton partial pressure equation.

$$\begin{aligned} &[O_2] \leftrightarrow [2O] \\ &[N_2] + [O] \leftrightarrow [NO] + [N] \\ &[N] + [O_2] \leftrightarrow [NO] + [O] \end{aligned} \quad (16)$$

$$\frac{d[NO]}{d\theta} = \frac{P \times 2.333 \times 10^{-7}.e^{\frac{38020}{T_b}}[N_2]_e.[O]_e.\left\{1 - \left(\frac{[NO]}{[NO]_e}\right)^2\right\}}{RT_b.\left(1 + \frac{2365}{T_b}.e^{\frac{2365}{T_b}}.\frac{[NO]}{[NO]_e}\right)}.\frac{1}{\omega} \quad (17)$$

The NO concentration in a cylinder is given by:

$$r_{NO_c} = r_{NO} r_{bc} \quad (18)$$

The specific NO in g/kWh is calculated as follows:

$$e_{NO} = \frac{30 \times r_{NO} \times M_{bg}}{L_C \times \eta_M} \quad (19)$$

Soot formation

Unburned hydrocarbons cause soot to form in diesel engines, posing a serious health risk and polluting the environment. The Hatridge smoke level may be used to calculate soot production [20,21]. The equation is used to calculate the generation of soot in the burning zone.

$$\left(\frac{d[C]}{dt}\right)_K = 0.004\frac{q_c}{V}\frac{dx}{dt} \quad (20)$$

$$\text{Hartridge} = 100\{1 - 0.9545\exp(-2.4226[C])\} \quad (21)$$

The Diesel-RK programmed uses equation (22) to determine the particulate matter by way of the meaning of Bosch-Number.

$$[PM] = 565\left(\ln\frac{10}{10 - BN}\right)^{1.206} \quad (22)$$

Validation of tool

To implement the Diesel RK-model numerical tool in the present investigation, an appropriate validation is mandatory. Hence, a comparative analysis is made between the data attained by experimentation and numerical tool. Fig. 2 compares experimental and numerically determined cylinder pressure and NO_X exhaust levels. With CR, the change in-cylinder pressure and NO_X emissions followed the same trend in both experimental and computational tests (Fig. 2).

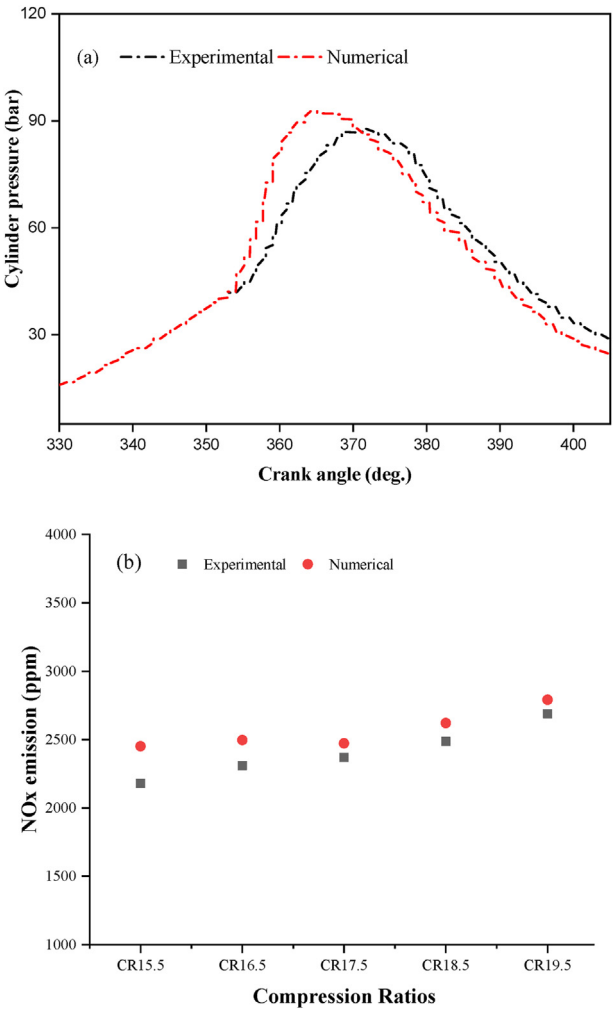

Fig. 2 – Tool validation with cylinder pressure vs. crank angle (a) and NOx emission (b) at different CRs.

Please cite this article as: Rajak U et al., Numerical and experimental investigation of hydrogen enrichment in a dual-fueled CI engine: A detailed combustion, performance, and emission discussion, International Journal of Hydrogen Energy, https://doi.org/10.1016/j.ijhydene.2022.07.144

The discrepancy between the values of these studies is in the range of 5.01 to 4.2%. Thus, from this comparative investigation, it is concluded that the adoption of the Diesel RK-software numerical tool is reasonably precise for further investigation.

Results and discussion

Cylinder pressure

One of the most critical combustion factors in an internal ignition machine is the highest combustion pressure. Fig. 3 shows the highest combustion pressure of the four investigated fuels (5H295BD, 5H295DEE, 5H295nB, and BD100) at five changed compression ratios (CR): 15.5, 16.5, 17.5, 18.5, and 19.5. In general, two different trends are observed in Fig. 3. Both 5H295BD and 5H295nB show a steady increase in the peak cylinder pressure with the increased compression ratio, while $5H_2$D95EE and BD100 show nearly the same trend except that they experience reduction at a certain compression ratio before increasing once again. At the highest CR 19.5, all the energy shows the highest peak cylinder pressure with the exception of 5H295DEE where its highest value (136 bar) is given at CR 19.5. The in-cylinder pressure delivery is only marginally impacted by raising the CR when there is a high load. With the CR, the peak cylinder pressure rose. This is primarily because there was significantly more trapped flammable gas under the high-load condition. The benefits of raising the CR were consistent with the high load because the in-cylinder temperature and pressure at the end of the compression stroke were also substantially higher at the high load [53,54].

On the other hand, the lowest peak in-cylinder pressure of all (70.9 bar) is given by 5H295nB at CR 15.5. The reason for the lowest peak in-cylinder pressure of 5H295nB at CR 15.5 could be due to the cooling effect of n-butanol resulting from its relatively high latent heat of vaporization, thus reducing the highest combustion temperature. Also, note that the low compression ratio is known to have relatively low temperature as a result of its increased clearance volume [43–45]. Therefore, the cooling effect of n-butanol coupled with lower temperature resulting from the use of a low compression ratio resulted in the most reduction of highest combustion pressure for $5H_2$ 95 nB at CR 15.5.

Brake thermal efficiency

The ratio of brake power (BP) to heat input (BD100) with five different compression ratios is known as braking thermal efficiency (BTE) (15.5, 16.5, 17.5, 18.5, and 19.5) in Fig. 4. Despite slight fluctuation given by BD100 and 5H295DEE, all fuels show minor variation in BTE with the increased compression ratio. The BTE at the lowest and the lowest compression ratios of such fuel were 34.08 and 28.47%, respectively. The difference is around 11%, thus considered as significant. Notably, for all compression ratios, 5H295nB consistently gives the greatest BTE, whereas 5H295DEE always gives the lowest. Specifically, the highest BTE (36.9%) is given by 5H295nB at CR 19.5, while the lowest BTE (28.47%) is given by 5H295DEE at CR 15.5. With the addition of hydrogen as a source of energy, thermal efficiency was improved due to more thorough combustion [40].

Brake-specific fuel consumption

The efficiency of an internal combustion engine is measured by brake-specific fuel consumption (BSFC). The BSFC is determined by dividing the fuel consumption rate (g/h) by the brake power produced (kW), yielding a unit in g/kWh. Fig. 5 shows the specific fuel consumption of fuels (5H295BD, 5H295DEE, 5H295nB and BD100) at five changed compression-ratios: 15.5, 16.5, 17.5, 18.5 and 19.5. Insignificant alterations are seen for 5H295nB and 5H295BD. The lowest BSFC is consistently provided by 5H295BD, whereas the greatest BSFC is regularly provided by 5H295DEE. Particularly, 5H295DEE at CR 17.5 provides the highest BSFC (333.45 g/kWh), whereas 5H295BD at CR 15.5 provides the lowest BSFC (231.84 g/kWh). The high cetane number of diethyl ether may have contributed to the maximum SFC supplied by 5H295DEE, which led to a shorter ignition delay and negatively impacted the fraternization process between the energy and the air. The outcome

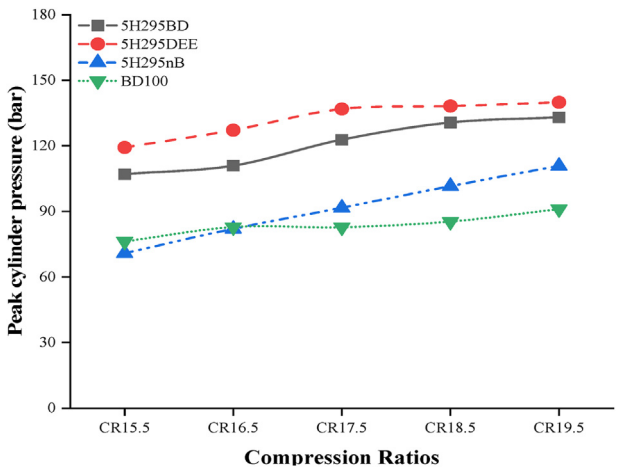

Fig. 3 – Peak cylinder pressure vs. compression ratios.

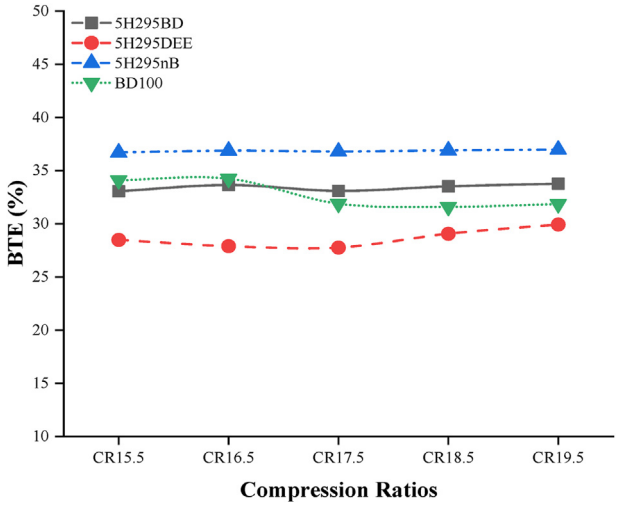

Fig. 4 – BTE vs. compression ratios.

Please cite this article as: Rajak U et al., Numerical and experimental investigation of hydrogen enrichment in a dual-fueled CI engine: A detailed combustion, performance, and emission discussion, International Journal of Hydrogen Energy, https://doi.org/10.1016/j.ijhydene.2022.07.144

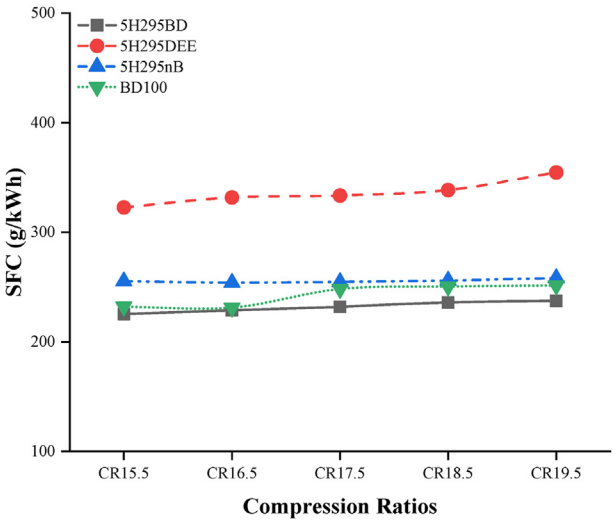

Fig. 5 – BSFC vs. compression ratios.

of adding diethyl ether to diesel fuel was a greater fuel consumption rate. By using hydrogen energy, particular fuel utilization is decreased at each compression ratio. Hydrogen reduces fuel consumption since it has a calorific value that is three times higher than base diesel [37,24,46].

Exhaust gas temperature

EGT is an exhaust gas temperature measurement at the exhaust manifold. Since it varies with the air-fuel ratio, it can be therefore used to control the mixture between the air and fuel flowing into the cylinder. Fig. 6 shows the exhaust gas temperature of the four investigated fuels (5H295BD, 5H295DEE, 5H295nB, and BD100) at five changed compression ratios: 15.5, 16.5, 17.5, 18.5, and 19.5. No significant variations are shown for all the fuels throughout the entire compression ratios.

The highest EGT is consistently given by BD100, whereas that of the lowest is always given by 5H295DEE. Specifically, the highest EGT (792.66 K) is given by BD100 at CR 17.5, while the lowest EGT (630.79 K) is given by 5H295DEE at CR 19.5. Therefore, the difference between the highest (792.66 K) and lowest EGT (630.79 K) is around 26%. Due to improved combustion characteristics brought on by higher combustion temperature and pressure, the BTE increased, even more, resulting in a higher CR. This was explained by a more efficient combustion process in dual-fuel mode, which was followed by an increase in the combustion temperature inside the machine chamber [31].

Ignition delay

The ignition delay in a compression explosion machine refers to the old-fashioned flinch of inoculation and the onset of combustion. The ignition delay of the four examined fuels (5H295BD, 5H295DEE, 5H295nB, and BD100) is shown in Fig. 7 for five changed compression ratios: 15.5, 16.5, 17.5, 18.5, and 19.5. With the increasing compression ratios, three fuels 5H295BD, 5H295nB, and BD100 show an analogous decreasing trend. The longest ignition delay is consistently given by 5H295nB, whereas that of the shortest is always given by 5H295DEE. Specifically, the longest ignition delay (15.028 deg.) is given by 5H295nB at CR 15.5, while the shortest (2.1677 deg.) is given by 5H295DEE at CR 19.5. Therefore, the difference between the longest (15.028 deg.) and shortest ignition delay (2.1677 deg.) is considerably significant. 5H295DEE has the least ignition delay of all examined fuels outstanding to its high cetane number. In addition to that, the higher compression ratio is known to increase the in-cylinder temperature that in turn could further shorten the ignition delay [47–49].

Therefore, the shortest ignition delay was given by fuel with the highest cetane number (5H295DEE) at the highest compression ratio (CR 19.5). Furthermore, note that at CR 15.5, the difference of ignition delay between fuel that produced the longest and the shortest ID is around. However, as the compression ratio is increasing, the discrepancy between those two values becomes smaller, reducing at CR 19.5 with no significant reduction observed for the addition of 5.0% diethyl ether.

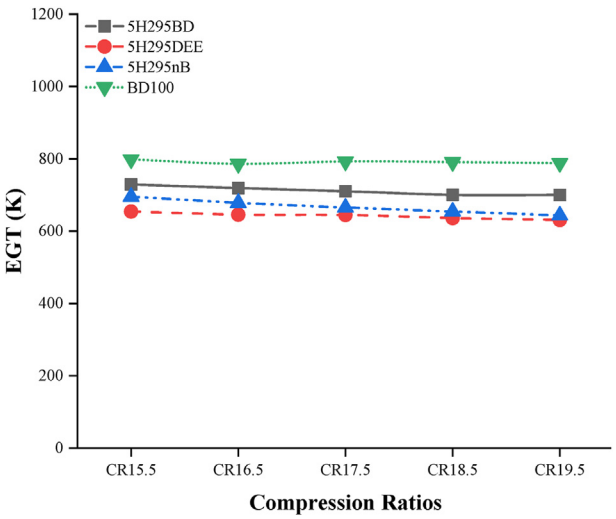

Fig. 6 – EGT vs. compression ratios.

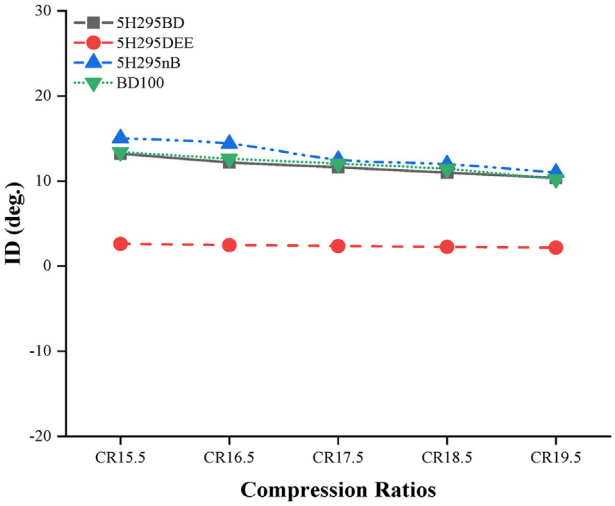

Fig. 7 – ID vs. compression ratios.

Please cite this article as: Rajak U et al., Numerical and experimental investigation of hydrogen enrichment in a dual-fueled CI engine: A detailed combustion, performance, and emission discussion, International Journal of Hydrogen Energy, https://doi.org/10.1016/j.ijhydene.2022.07.144

Carbon dioxide emissions

Carbon Dioxide (CO_2) is a colorless, incombustible, and odorless gas produced from carbon oxidation. Extra CO_2 in the atmosphere raises the greenhouse effect, trapping radiation and creating ozone at ground level, thus preventing the earth from cooling. Fig. 8 shows the CO_2 of the four investigated fuels (5H295BD, 5H295DEE, 5H295nB and BD100) at five changed compression-ratios: 15.5, 16.5, 17.5, 18.5 and 19.5. No significant variations are shown for all the fuels throughout the entire compression ratios. The highest CO_2 is consistently given by BD100, whereas that of the lowest is always given by 5H295nB. Specifically, the highest CO_2 (815.5 g/kWh) is given by BD100 at CR 19.5, while the lowest CO_2 (581.31 g/kWh) is given by 5H295nB; were at CR 15.5. Therefore, the difference between the highest and lowest CO_2 is only around 28.71%.

The fact that 5H295nB produced the lowest level of CO_2 emission could be due to its lower calorific value and higher density for obtaining the same engine power output, thus releasing less energy. It is known that CO_2 emission decreases with an increase in BTE. Referring to BTE results discussed previously in which 5H295nB has the highest BTE of all the investigated fuels, the trend of CO_2 emission presented in Fig. 8 clearly confirms the inverse relationship between BTE and CO_2 emissions. The deficiency of carbon atoms in hydrogen, greater hydrogen/carbon ratio, littler ignition time, and improved combustion efficiency are all reasonable origins of lower CO_2 levels. In other words, using hydrogen reduces the amount of carbon available in the combustion [50].

Smoke emissions

In compression ignition engines, smoke emission is greatly dependent on fuel atomization and O_2 deficiency. Fig. 9 shows the smoke emissions of the four investigated fuels (5H295BD, 5H295DEE, 5H295nB, and BD100) at five changed compression ratios: 15.5, 16.5, 17.5, 18.5, and 19.5. Almost on par trend is given by 5H295DEE and BD100. No significant change in smoke emission is produced by 5H295BD throughout all compression ratios, while a steady decrease is given by 5H295nB. The highest

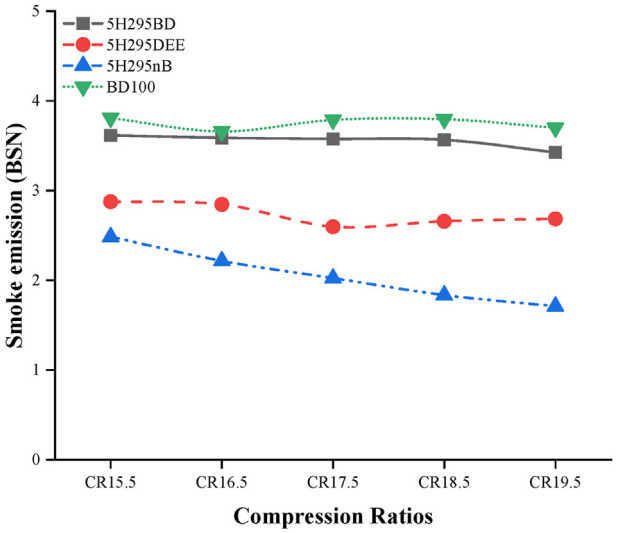

Fig. 9 – Smoke emission vs. compression ratios.

smoke emission is given by BD100 (3.78 BSN), whereas that of the lowest is given by 5H295nB (1.7105 BSN); both were at CR 19.5. Therefore, the difference between the highest (3.7989 BSN) and lowest smoke emission (1.7105 BSN) is around 122%. The addition of 5% hydrogen is the only blend that shows a consistent decrease with the increasing compression ratio. This tendency could be attributed to its lower carbon and higher oxygen content. Also, a higher compression ratio was believed to enhance the air density and in-cylinder temperature, foremost to improve fuel/air fraternization, which promoted more complete combustion, thus reducing smoke emissions. Similar results were reported in Refs. [25–27].

Oxides of nitrogen emissions

The NO_X emission formation greatly depends on the maximum temperature of the gases inside the fire chamber as well as the reaction time available. Fig. 10 shows the NO_X emission of the four investigated fuels (5H295BD, 5H295DEE,

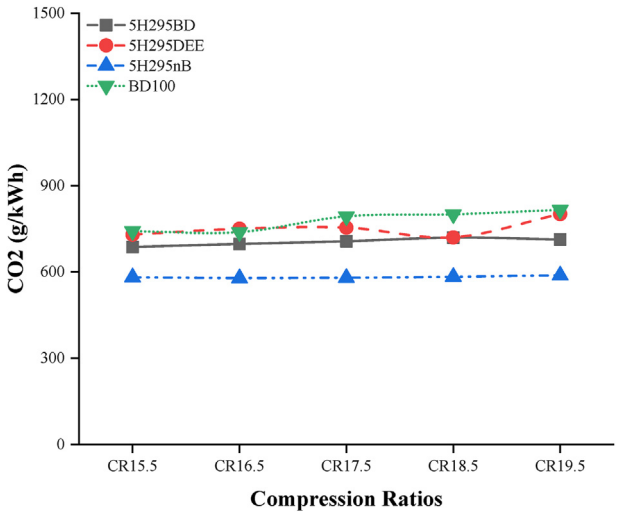

Fig. 8 – Carbon dioxide emission vs. compression ratios.

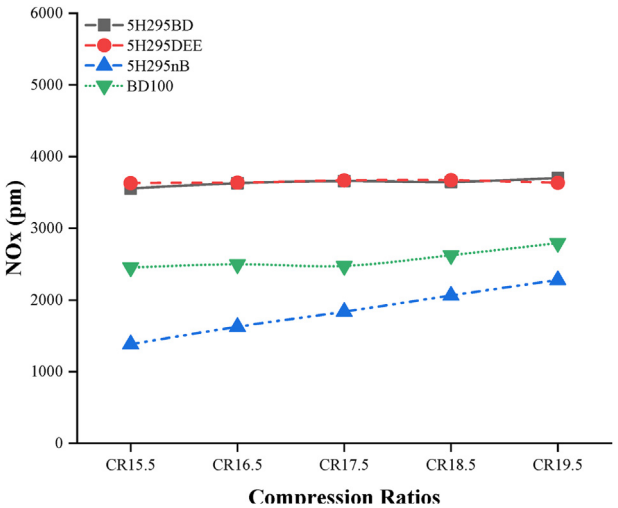

Fig. 10 – NO_X vs. compression ratios.

Please cite this article as: Rajak U et al., Numerical and experimental investigation of hydrogen enrichment in a dual-fueled CI engine: A detailed combustion, performance, and emission discussion, International Journal of Hydrogen Energy, https://doi.org/10.1016/j.ijhydene.2022.07.144

5H295nB and BD100) at five changed compression-ratios: 15.5, 16.5, 17.5, 18.5 and 19.5. Both 5H295BD and 5H295DEE experience a comparable trend as the compression ratio is increasing from 15.5 to 19.5. Nearly the same trend is observed for BD100. Interestingly, unlike other fuels whose level of NOx emission was at the lowest compression ratio, 5H295BD shows a gradual increase with the highest NOx level produced at CR 19.5. The highest NOx emission (3697.9 ppm) is given by 5H295BD at CR 19.5, whereas that of the lowest (1924.8 ppm) is given by 5H295nB at CR 15.5. The lowest NOx emission given by 5H295nB at CR15.5 could be due to its longest ignition delay as mentioned previously. This led to less residual gas and wall temperature, thus reducing the NOx emission. This is in agreement with previous results reported by Venu and Madhavan [28]. N-butanol's high latent heat of vaporization and its cooling effect may also be the reasons for such NOx reduction. High oxygen concentration has an impact on NOx generation. However, alternative fuel has a lower heating value than diesel fuel, and its high moisture content also contributed to lessened NOx generation. Alternative fuel's high moisture content absorbs combustion heat and lowers post-combustion temperatures. The reaction between nitrogen and oxygen molecules was slowed considerably by this situation. The load grew along with the amount of fuel injected, which also raised the post-combustion temperature and NOx emissions. With CR, the NOx emission rose [53,54].

Note that at CR 15.5, the difference in NOx level between fuel that produced the highest and the lowest value is around 56%. This is because as the compression ratio increased, the clearance volume decreased, raising the pressure and temperature inside the cylinder and compensating for the cooling impact of n-high butanol latent heat of vaporization. One possible explanation for the spike in NOx levels is a greater flame temperature of hydrogen in the cylinder [30,51].

PM emissions

Particulate Matter (PM) is a combination of liquid droplets and solid particles floating in the atmosphere. Exposure to PM can severely affect both lungs and heart, causing premature death. Fig. 11 shows the PM emissions of the four investigated fuels (5H295BD, 5H295DEE, 5H295nB and BD100) at five changed compression-ratios: 15.5, 16.5, 17.5, 18.5 and 19.5. Each fuel shows a different trend throughout the entire compression ratio. In most cases, the highest PM emission was produced by BD100, while that of the lowest was emitted by 5H295nB. Specifically, the highest PM emission (0.86 g/kWh) was given by BD100 at CR19.5, while the lowest (0.47 g/kWh) was given by 5H295nB; at CR 15.5. Therefore, the difference between the highest (0.86 g/kWh) and lowest PM emission (0.47 g/kWh) is 45.3%. However, as the compression ratio is increasing, the discrepancy between those two values becomes significantly bigger at CR 19.5. Significant PM reduction given by 5H295nB at CR 19.5 could be attributed to the increased in-cylinder temperatures resulting from a high compression ratio, thus promoting post-combustion oxidation. The extra oxygen content in n-butanol further facilitated more complete combustion, thus helping to reduce the PM emissions [40]. Hence, a higher in-cylinder resulting from a high compression ratio along with n-butanol extra O_2 content resulted in significant PM emission reduction for 5H295nB at CR 19.5.

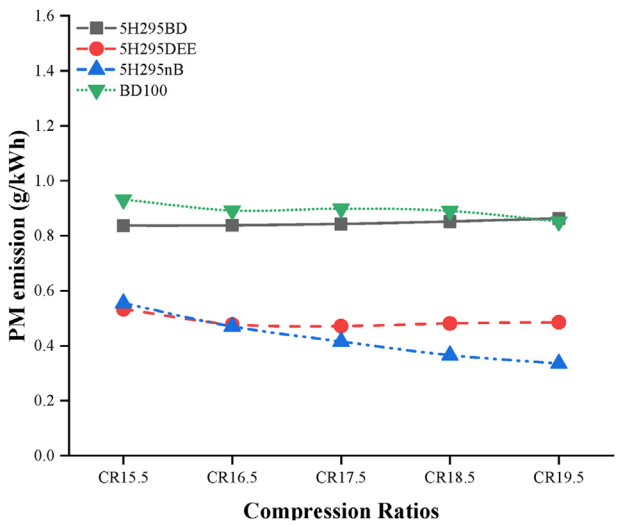

Fig. 11 – PM vs. compression ratios.

Conclusion

Using 5% hydrogen energy sharing with base diesel, diethyl ether extraction at various compression ratios was investigated (CR15.5-CR19.5). The study's findings are presented below:

- All the tested blends, which peaked at CR 19.5, and all analyzed fuels demonstrated the highest in-cylinder peak pressure in the study's increase in peak cylinder pressure with increasing compression ratio.
- Although BD100 and 5H295DEE showed some modest fluctuation, all fuels displayed negligible changes in BTE as the compression ratio increased. 5H295nB consistently gave the highest BTE, while 5H295DEE consistently delivered the lowest.
- The BSFC tended to rise along with the increase in engine CRs. Additionally, the BSFC's tendency to use hydrogen energy to base diesel was significantly diminished. No significant disparities in EGT were shown for all the fuels. The highest temperature of exhaust gas was 792.66 K given by BD100 at CR 17.5, while the lowest EGT was 630.79 K provided by 5H295DEE at CR 19.5.
- Three fuels—5H295BD, 5H295nB, and BD100—showed an identical decreasing tendency in terms of the ignition delay, while 5H295DEE saw minimal alterations. 5H295DEE consistently provided the ignition delay with the shortest time.
- BD100 displayed the highest CO_2 (802.85 g/kWh), while 5H295nB displayed the lowest CO_2 (578.61 g/kWh); both were at CR 19.5. Therefore, there wasn't much of a difference in CO_2 between the highest (802.85 g/kWh) and lowest (578.61 g/kWh), only about 39%.
- With an increase in CR from 15:5 to 19.5, hazardous NOx emission steadily improved. Due to increased combustion

Please cite this article as: Rajak U et al., Numerical and experimental investigation of hydrogen enrichment in a dual-fueled CI engine: A detailed combustion, performance, and emission discussion, International Journal of Hydrogen Energy, https://doi.org/10.1016/j.ijhydene.2022.07.144

pressure and temperature, higher CR was associated with higher NOx production.
- Each fuel displayed a distinct pattern in terms of PM emissions over the course of all compression ratios. Most of the time, BD100 produced the highest PM emissions, awhereas 5H295nB produced the lowest.

Declaration of competing interest

The authors declare that they have no known competing financial interests or personal relationships that could have appeared to influence the work reported in this paper.

Acknowledgments

The authors appreciate the help they received from RGM College of Engineering and Technology Nandyal and Maulana Azad National Institute of Technology Bhopal, MP.

Abbreviation

BD100	Base diesel fuel 100%
5H295BD	5% hydrogen and 95% base diesel
5H295DEE	5% hydrogen and 95% diethyl ether
5H295nB	5% hydrogen and 95% n-Butanol
rpm	Revolution per minute
CR	Compression ratio
BTE	Brake thermal efficiency
BSFC	Brake specific fuel consumption
MPRR	Maximum pressure rise rate
CO_2	Carbon dioxide
NO_x	Oxides of nitrogen
PM	Particulate matter
EGT	Exhaust gas temperature
ID	Ignition delay
A_0, A_1, A_2	Empirical factors
BN	Bosch number
$\dot{S}_g$	Net generation rate of the ith species (kg/sec)
E_a	Apparent activation energy for the auto ignition process (kJ/kmole)
T_b	temperature in a burnt gas zone (K)
V_i and V_c	Cylinder volumes at injection timing and top dead centre (cm^3)
x	Fraction of fuel burnt
X_0	Fraction of burnt fuel during ignition delay
Y_i	Mass fraction
K_T	Evaporation constant
$[N_2]_e$	Equilibrium concentrations of an molecular nitrogen
$[NO]_e$	Equilibrium concentrations of an oxide of nitrogen
$[O]_e$	Equilibrium concentrations of molecular oxygen
$[O_2]_e$	Equilibrium concentrations of atomic oxygen
Y_i^{cyl}	Stoichiometric coefficients on the reactant side
Y_i^j	Stoichiometric coefficients on the product side
α_1	Air-fuel equivalence ratio
τ	Time (second)
ρ	Density (kg/m^3)
ν	Specific volume (m^3/kg)
φ	Crank angle (degree)
ω	Angular crank velocity (rpm)
ξ_b	Cylinder air charge usage efficiency
σ_{ud}	σ_u Fuel fractions evaporated during ignition delay period and up

REFERENCES

[1] Dimitriou P, Tsujimura T, Suzuki Y. Adopting biodiesel as an indirect way to reduce the NOx emission of a hydrogen fumigated dual-fuel engine. Fuel May 2019;244:324–34. https://doi.org/10.1016/j.fuel.2019.02.010.

[2] Kanth S, Debbarma S. Comparative performance analysis of diesel engine fuelled with hydrogen enriched edible and non-edible biodiesel. Int J Hydrogen Energy Mar. 2021;46(17):10478–93. https://doi.org/10.1016/j.ijhydene.2020.10.173.

[3] Loganathan M, Madhavan VM, Arun Balasubramanian K, Thanigaivelan V, Vikneswaran M, et al. Investigation on the effect of diethyl ether with hydrogen-enriched cashew nut shell (CNS) biodiesel in direct injection (DI) diesel engine. Fuel Oct. 2020;277:118165. https://doi.org/10.1016/j.fuel.2020.118165.

[4] Çalık A. Determination of vibration characteristics of a compression ignition engine operated by hydrogen enriched diesel and biodiesel fuels. Fuel Oct. 2018;230:355–8. https://doi.org/10.1016/j.fuel.2018.05.053.

[5] Khan MB, Kazim AH, Farooq M, Javed K, Shabbir A, et al. Impact of HHO gas enrichment and high purity biodiesel on the performance of a 315 cc diesel engine. Int J Hydrogen Energy May 2021;46(37):19633–44. https://doi.org/10.1016/j.ijhydene.2021.03.112.

[6] Manigandan S, Ponnusamy VK, Devi PB, Oke SA, Sohret Y, et al. Effect of nanoparticles and hydrogen on combustion performance and exhaust emission of corn blended biodiesel in compression ignition engine with advanced timing. Int J Hydrogen Energy Jan. 2020;45(4):3327–39. https://doi.org/10.1016/j.ijhydene.2019.11.172.

[7] Elkelawy M, Etaiw SEH, Alm-Eldin Bastawissi H, Ayad MI, Radwan AM, et al. Diesel/biodiesel/silver thiocyanate nanoparticles/hydrogen peroxide blends as new fuel for enhancement of performance, combustion, and Emission characteristics of a diesel engine. Energy Feb. 2021;216:119284. https://doi.org/10.1016/j.energy.2020.119284.

[8] Saidi M, Moradi P. Conversion of biodiesel synthesis waste to hydrogen in membrane reactor: theoretical study of glycerol steam reforming. Int J Hydrogen Energy Mar. 2020;45(15):8715–26. https://doi.org/10.1016/j.ijhydene.2020.01.064.

[9] Sui M, Chen Y, Li F, Wang W, Shen J. Study on the mechanism of auto-oxidation of Jatropha biodiesel and the oxidative cleavage of C C bond. Fuel May 2021;291:120052. https://doi.org/10.1016/j.fuel.2020.120052.

[10] Adu-Mensah D, Mei D, Zuo L, Zhang Q, Wang J. A review on partial hydrogenation of biodiesel and its influence on fuel properties. Fuel Sep. 2019;251:660–8. https://doi.org/10.1016/j.fuel.2019.04.036.

[11] Sukjit E, Tongroon M, Chollacoop N, Yoshimura Y, Poapongsakorn P, et al. Improvement of the tribological behaviour of palm biodiesel via partial hydrogenation of unsaturated fatty acid methyl esters. Wear Apr. 2019;426–427:813–8. https://doi.org/10.1016/j.wear.2018.12.017.

Please cite this article as: Rajak U et al., Numerical and experimental investigation of hydrogen enrichment in a dual-fueled CI engine: A detailed combustion, performance, and emission discussion, International Journal of Hydrogen Energy, https://doi.org/10.1016/j.ijhydene.2022.07.144

[12] Meng Q, Lin X, Zhai Y, Zhang L, Zhang P, et al. A theoretical investigation on Bell-Evans-Polanyi correlations for hydrogen abstraction reactions of large biodiesel molecules by H and OH radicals. Combust Flame Apr. 2020;214:394–406. https://doi.org/10.1016/j.combustflame.2020.01.005.
[13] Chacko N, Johnson C, Varadarajan P, Sai Srinivas S, Jeyaseelan T. A comparative evaluation of cetane enhancing techniques for improving the smoke, NOx and BSFC trade-off in an automotive diesel engine. Fuel Apr. 2021;289:119918. https://doi.org/10.1016/j.fuel.2020.119918.
[14] Zhu T, Zhang L, Li Z, Wei G, Xin Z, et al. Synthesis of bentonite-based nickel catalyst using [Ni(NH3)6](NO3)2 as precursor for enhanced hydrogenation of biodiesel. Mater Lett Dec. 2019;256:126585. https://doi.org/10.1016/j.matlet.2019.126585.
[15] Wang Y, Zhou X, Liu L. Theoretical investigation of the combustion performance of ammonia/hydrogen mixtures on a marine diesel engine. Int J Hydrogen Energy Apr. 2021;46(27):14805–12. https://doi.org/10.1016/j.ijhydene.2021.01.233.
[16] Wang Z, Zhang F, Xia Y, Wang D, Xu Y, et al. Combustion phase of a diesel/natural gas dual fuel engine under various pilot diesel injection timings. Fuel Apr. 2021;289:119869. https://doi.org/10.1016/j.fuel.2020.119869.
[17] Veza I, Faizullizam Roslan M, Farid Muhamad Said M, Abdul Latiff Z, Azman Abas M. Physico-chemical properties of Acetone-Butanol-Ethanol (ABE)-diesel blends: blending strategies and mathematical correlations. Fuel Feb. 2021;286:119467. https://doi.org/10.1016/j.fuel.2020.119467.
[18] Veza I, Said MFM, Latiff ZA. Progress of acetone-butanol-ethanol (ABE) as biofuel in gasoline and diesel engine: a review. Fuel Process Technol Dec. 2019;196:106179. https://doi.org/10.1016/j.fuproc.2019.106179.
[19] Veza I, Muhamad Said MF, Latiff ZA. Recent advances in butanol production by acetone-butanol-ethanol (ABE) fermentation. Biomass Bioenergy Jan. 2021;144:105919. https://doi.org/10.1016/j.biombioe.2020.105919.
[20] Saleh HE. Performance and emissions characteristics of direct injection diesel engine fueled by diesel-jojoba oil-butanol blends with hydrogen peroxide. Fuel Feb. 2021;285:119048. https://doi.org/10.1016/j.fuel.2020.119048.
[21] Kumar CB, Lata DB. Effect of di-tert butyl peroxide (DTBP) on combustion parameters and NOx in dual fuel diesel engine with hydrogen as a secondary fuel. Int J Hydrogen Energy Jan. 2021;46(5):4507–25. https://doi.org/10.1016/j.ijhydene.2020.10.235.
[22] Polat F. Performance and emission behaviors of a CI engine fueled by waste feedstocks at varying compression ratios. Proc IME E J Process Mech Eng 2022:09544089221074845. https://doi.org/10.1177/09544089221074845. In press.
[23] Polat F. Experimental evaluation of the impacts of diesel-nanoparticles-waste tire pyrolysis oil ternary blends on the combustion, performance, and emission characteristics of a diesel engine. Process Saf Environ Protect 2022;160:847–58. https://doi.org/10.1016/j.psep.2022.03.003.
[24] Khandal SV, Ağbulut Ü, Afzal A, Sharifpur M, Abdul Razak K, Khalilpoor N. Influences of hydrogen addition from different dual-fuel modes on engine behaviors. Energy Sci Eng 2022;10(3):881–91. https://doi.org/10.1002/ese3.1065.
[25] Gunasekar P, Manigandan S, V.S., Gokulnath R, Vimal R, et al. Effect of hydrogen addition on exergetic performance of gas turbine engine. Aircraft Eng Aero Technol Oct. 2019;92(2):180–5. https://doi.org/10.1108/AEAT-05-2019-0095.
[26] Akdeniz HY, Balli O. Energetic and exergetic assessment of operating biofuel, hydrogen and conventional JP-8 in a J69 type of aircraft turbojet engine. J Therm Anal Calorim Nov. 2021;146(4):1709–21. https://doi.org/10.1007/s10973-021-10879-z.
[27] Gürbüz H, Şöhret Y, Akçay H. Environmental and enviroeconomic assessment of an LPG fueled SI engine at partial load. J Environ Manag Jul. 2019;241:631–6. https://doi.org/10.1016/j.jenvman.2019.02.113.
[28] Gürbüz H, Akçay İH. Evaluating the effects of boosting intake-air pressure on the performance and environmental-economic indicators in a hydrogen-fueled SI engine. Int J Hydrogen Energy Aug. 2021;46(56):28801–10. https://doi.org/10.1016/j.ijhydene.2021.06.099.
[30] Zhang X, Yang R, Anburajan P, Van Le Q, Alsehli M, et al. Assessment of hydrogen and nanoparticles blended biodiesel on the diesel engine performance and emission characteristics. Fuel Jan. 2022;307:121780. https://doi.org/10.1016/j.fuel.2021.121780.
[31] Rosha P, Kumar S, Senthil Kumar P, Kowthaman CN, Kumar Mohapatra S, et al. Impact of compression ratio on combustion behavior of hydrogen enriched biogas-diesel operated CI engine. Fuel Feb. 2022;310:122321. https://doi.org/10.1016/j.fuel.2021.122321.
[34] Mabadi Rahimi H, Jazayeri SA, Ebrahimi M. Hydrogen energy share enhancement in a heavy duty diesel engine under RCCI combustion fueled with natural gas and diesel oil. Int J Hydrogen Energy Jul. 2020;45(35):17975–91. https://doi.org/10.1016/j.ijhydene.2020.04.263.
[35] The U.S. Energy information administration (EIA), "annual energy outlook 2019 with projections to 2050 [Online]. Available: https://www.biomassmurder.org/docs/2019-03-05-eia-annual-energy-outlook-2019-with-projections-to-2050-english.pdf; 2019.
[36] Ghazal OH. Combustion analysis of hydrogen-diesel dual fuel engine with water injection technique. Case Stud Therm Eng Mar. 2019;13:100380. https://doi.org/10.1016/j.csite.2018.100380.
[37] Gürbüz H, Akçay H, Aldemir M, Akçay İH, Topalcı Ü. The effect of euro diesel-hydrogen dual fuel combustion on performance and environmental-economic indicators in a small UAV turbojet engine. Fuel Dec. 2021;306:121735. https://doi.org/10.1016/j.fuel.2021.121735.
[38] Singh TS, Rajak U, Dasore A, Muthukumar M, Verma TN. Performance and ecological parameters of a diesel engine fueled with diesel and plastic pyrolyzed oil (PPO) at variable working parameters. Environ Technol Innovat May 2021;22:101491. https://doi.org/10.1016/j.eti.2021.101491.
[39] Rajak U, Chaurasiya PK, Nashine P, Verma M, Reddy Kota T, et al. Financial assessment, performance and emission analysis of Moringa oleifera and Jatropha curcas methyl ester fuel blends in a single-cylinder diesel engine. Energy Convers Manag Nov. 2020;224:113362. https://doi.org/10.1016/j.enconman.2020.113362.
[40] Rajak U, Nashine P, Verma TN, Pugazhendhi A. Performance and emission analysis of a diesel engine using hydrogen enriched n-butanol, diethyl ester and Spirulina microalgae biodiesel. Fuel Jul. 2020;271:117645. https://doi.org/10.1016/j.fuel.2020.117645.
[41] Kuleshov AS. Model for predicting air-fuel mixing, combustion and emissions in DI diesel engines over whole operating range. In: SAE technical paper 2005-01-2119; May 2005. p. 17. https://doi.org/10.4271/2005-01-2119.
[42] Kuleshov AS. Multi-zone DI diesel spray combustion model for thermodynamic simulation of engine with PCCI and high EGR level. SAE International Journal of Engines Jun. 2009;2(1). https://doi.org/10.4271/2009-01-1956. 2009-01–1956.
[43] Kalil Rahiman M, Santhoshkumar S, Subramaniam D, Avinash A, Pugazhendhi A. Effects of oxygenated fuel pertaining to fuel analysis on diesel engine combustion and emission characteristics. Energy Jan. 2022;239:122373. https://doi.org/10.1016/j.energy.2021.122373.

Please cite this article as: Rajak U et al., Numerical and experimental investigation of hydrogen enrichment in a dual-fueled CI engine: A detailed combustion, performance, and emission discussion, International Journal of Hydrogen Energy, https://doi.org/10.1016/j.ijhydene.2022.07.144

[44] Kocakulak T, Babagiray M, Nacak Ç, Safieddin Ardebili SM, Calam A, et al. Multi objective optimization of HCCI combustion fuelled with fusel oil and n-heptane blends. Renew Energy Jan. 2022;182:827–41. https://doi.org/10.1016/j.renene.2021.10.041.
[45] Akcay M, Yilmaz IT, Feyzioglu A. The influence of hydrogen addition on the combustion characteristics of a common-rail CI engine fueled with waste cooking oil biodiesel/diesel blends. Fuel Process Technol Dec. 2021;223:106999. https://doi.org/10.1016/j.fuproc.2021.106999.
[46] Wu H-W, Wu Z-Y. Investigation on combustion characteristics and emissions of diesel/hydrogen mixtures by using energy-share method in a diesel engine. Appl Therm Eng Sep. 2012;42:154–62. https://doi.org/10.1016/j.applthermaleng.2012.03.004.
[47] Nag S, Dhar A, Gupta A. Hydrogen-diesel co-combustion characteristics, vibro-acoustics and unregulated emissions in EGR assisted dual fuel engine. Fuel Jan. 2022;307:121925. https://doi.org/10.1016/j.fuel.2021.121925.
[48] Ansari E, Menucci T, Shahbakhti M, Naber J. Experimental investigation into effects of high reactive fuel on combustion and emission characteristics of the Diesel - natural gas Reactivity Controlled Compression Ignition engine. Appl Energy Apr. 2019;239:948–56. https://doi.org/10.1016/j.apenergy.2019.01.256.
[49] Babayev R, Andersson A, Serra Dalmau A, Im HG, Johansson B. Computational comparison of the conventional diesel and hydrogen direct-injection compression-ignition combustion engines. Fuel Jan. 2022;307:121909. https://doi.org/10.1016/j.fuel.2021.121909.
[50] Tosun E, Özcanlı M. Hydrogen enrichment effects on performance and emission characteristics of a diesel engine operated with diesel-soybean biodiesel blends with nanoparticle addition. Engineering Science and Technology, an International Journal Jun. 2021;24(3):648–54. https://doi.org/10.1016/j.jestch.2020.12.022.
[51] Zareei J, Haseeb M, Ghadamkheir K, Farkhondeh SA, Yazdani A, et al. The effect of hydrogen addition to compressed natural gas on performance and emissions of a DI diesel engine by a numerical study. Int J Hydrogen Energy Nov. 2020;45(58):34241–53. https://doi.org/10.1016/j.ijhydene.2020.09.027.
[53] Guo T, Duan X, Liu Y, Liu J, Zhou X, Li Y. A comparative experimental study on emission characteristics of a turbocharged gasoline direct-injection (TGDI) engine fuelled with gasoline/ethanol blends under transient cold-start and steady-state conditions. Fuel 2020;277(March):118153. https://doi.org/10.1016/j.fuel.2020.118153.
[54] Xu L, Sun X, Ku C, Liu J, Lai M, Duan X. Effects of control strategies for mixture activity and chemical reaction pathway coupled with exhaust gas recirculation on the performance of hydrogen-enriched natural-gas fueled spark ignition engine. Fuel 2022;322(March):124153. https://doi.org/10.1016/j.fuel.2022.124153.

Please cite this article as: Rajak U et al., Numerical and experimental investigation of hydrogen enrichment in a dual-fueled CI engine: A detailed combustion, performance, and emission discussion, International Journal of Hydrogen Energy, https://doi.org/10.1016/j.ijhydene.2022.07.144